The use of CaO:Eu^{3+} and Zn$_2$SiO$_4$:Mn^{2+} phosphors to increase the color quality and illumination intensity of WLEDs

Ho Minh Trung[1], My Hanh Nguyen Thi[2], Hoang Thinh Nhan[3]
[1]Faculty of Basic Sciences, Vinh Long University of Technology Education, Vinh Long Province, Vietnam
[2]Faculty of Mechanical Engineering, Industrial University of Ho Chi Minh City, Ho Chi Minh City, Vietnam
[3]Nguyen Tat Thanh University Innovation Incubation Center, Nguyen Tat Thanh University, Ho Chi Minh City, Vietnam

Article Info

ABSTRACT

The lumen efficacy in remote phosphor structure displayed remarkable enhancements, which is notable for the development of white light emitting diodes (WLEDs). Nevertheless, its quality of colour is deemed not as good as that of the conformal or in-cup phosphor structure. Therefore, the goal of this research is to achieve a better quality of colour and significant luminous flux value for remote phosphor configuration by using extra phosphor layers. In particular, the two-layer and three-layer structures with the implementation of green and red phosphors are proposed. Comparing these two structures can help pinpoint the best suited for the WLED production. The assessment of each structure's effect on the WLEDs' optical parameters was determined under various correlated temperatures of colour (5,600-8,500 K). The outcomes indicated that the three-layer structure enhanced the quality of colour with greater efficiency compared to the two-layer structure due to the increased color rendering index (CRI), color quality scale (CQS), and photoluminescence (PL), and reduced colour deviation. The scattering improvement of the three-layer structure is a key factor of these accomplishments, proven by the scattering theory of Mie. Therefore, the three-layer structure is potential for developing WLED production.

Corresponding Author:

My Hanh Nguyen Thi
Faculty of Mechanical Engineering, Industrial University of Ho Chi Minh City
No. 12 Nguyen Van Bao Street, Ho Chi Minh City, Vietnam
Email: nguyenthimyhanh@iuh.edu.vn

1. INTRODUCTION

The light emitting diodes (LEDs) firm groundwork has been contributing to the solid-state lighting (SSL) industry. The LEDs were considered appropriate replacements of the halogen, incandescent, and fluorescent lighting systems, thanks to the better safety and potency. Furthermore, researchers confirmed many benefits of LEDs: higher efficiency of energy conversion with the result of reduced heat release, higher lifetime, and reliable optical performance [1], [2]. In a standard way, a LED package was created through merging one blue chip with one yellow phosphor substance, resulting in the presence of yellow and blue light in LED light emitted [3]. Among the white light emitting diodes (WLEDs)-manufacturing methods, the most straightforward one with the most widespread application is the freely dispersed phosphor coating. The combination containing phosphor granules along with silicone was daubed on the blue chip in no particular pattern. This particular technique brings some benefits, which is the insignificant expense and configurable thickness of phosphor layer, while has the downside of the LED package's insignificant light efficiency, which means that it is unfit for the manufacture of high-power WLED [4]–[6]. The conformal phosphor application was subsequently proposed for enhancing the LEDs' performance. While this technique is

capable of delivering uniform colour distribution to colour uniformity, the backscattering inside the structure deteriorated the light extraction efficiency [7]–[9]. Moreover, the aforementioned techniques revolve around the placement of phosphorus film on the LED chip surface, which caused the rise in temperature at the junction and brought down the phosphor's efficacy and the LED's longevity. Therefore, researchers proposed a gap creation or the addition of an extra layer positioned between the primary phosphor-silicone setting and the chip of LED for the purpose of improving the light extraction and keeping the heat release at a minimal level [10]–[12]. The structure above was named the remote phosphor structure, which became a significant subject of many pieces of research intended to improve WLED's optical characteristics. An encapsulation, isolated from heat, was made to boost light output power through the manipulation of thermal release throughout a WLED's significant time of use [13]. Different methods were used to boost the light extraction efficacy in remote phosphor structure, such as utilizing the polymer hemispherical shell lens internally coated with phosphor to improve inner reflection [14], the structure implemented with an air gap to reflect downward light [15], and ring remote phosphor package to lower the light backscattering [16].

The light extraction efficacy has a great significance in the making of WLED of high quality. However, the quality of colour, which includes color rendering index (CRI) along with color quality scale (CQS), also has a similar role. The two-layer structure was proposed for the enhancement of the colour fullness as well as lumen efficacy. With the implementation of the two-sheet remote phosphor setting, the WLED's lumen output could be increased by 5% and the colour uniformity thanks to the considerable decrease in the angular colour deviation [8]. Still, the effectiveness of the two-layer phosphor structure is dependent on the extra layer of phosphor. Specifically, when the layer of red phosphor is added, the CRI increases, and the lumen is reduced. The results are reversed when red phosphor is replaced with green phosphor. Moreover, the earlier researches showed that the increased concentration of phosphor caused a higher reabsorption loss in the structure, resulting in a lower lumen [17], [18]. As a result, the use of an extra layer of phosphor could give promising results. The three-sheet remote phosphor setting, accompanied by phosphor layers in yellow, red, and green, was introduced. The layer of yellow phosphor (the layer which comes first) is placed nearest to the chip of LED, the green sheet comes in second, with the red sheet being the third. For this research, our main focus is the effectiveness of the three-sheet remote phosphor setting for the WLED's optical efficacy. The configuration for phosphor concentrations was made to examine the changes in illumination extrication, discharge spectrum, color aberration, CRI, as well as CQS of the packages [19], [20]. Furthermore, we compared the one-layer, two-layer, and three-layer remote packages to confirm the superiority of the three-layer package in improving LED's performance. The phosphor samples involved in the making of the phosphor structures of this research would be yellow-emitting $YAG:Ce^{3+}$, red-emitting $CaO:Eu^{3+}$, along with green-emitting $Zn_2SiO_4:Mn^{2+}$ phosphors. We also carried out measurements through the Mie-scattering hypothesis as well as Lambert-Beer law. Therefore, manufacturers can take advantage of the research's discoveries to select an appropriate remote phosphor structure for higher performances of WLED with high power.

2. METHOD
2.1. White light-emitting diodes simulation

Using the computer program LightTools 9.0, we simulated the models of four remote phosphor layer packages: one-layer remote phosphor structure, dual-sheet remote phosphor structures with red as well as green phosphors, and three-sheet structure, all demonstrated in Figure 1. We can achieve a higher colour quality through increasing the red spectrum with red phosphor $CaO:Eu^{3+}$, while the presence of green light in the white-light spectral power band can be increased by using green phosphor $Zn_2SiO_4:Mn^{2+}$ to achieve better lumen efficacy in the WLED. The WLED model simulated is the multi-chip WLED with nine blue chips bonded to the lead frame, shown in Figure 1(a). The chips have a radiant power of 1.16 W that peaks at 453 nm wavelength. Figure 1(b) provides further details of the WLED model. Figure 1(c) exhibits the one-sheet configuration accompanied by $YAG:Ce^{3+}$ phosphor layer (Y) implemented. Figure 1(d) displays the double-sheet setting accompanied by the yellow phosphor sheet and the extra red phosphor layer (YR). Figure 1(e) demonstrates the same structure in Figure 1(d) but now with the red phosphor layer replaced by green phosphor $Zn_2SiO_4:Mn^{2+}$ layer (YG). Figure 1(f) presents the three-layer structure with red and green phosphor layers (YRG). We optically examined the four structures mentioned above at five correlated color temperatures (CCTs): 5,600, 6,600, 7,000, 7,700, 8,500 K, and at various red, green-emitting phosphor concentrations. When the red or green phosphor changes in its concentration, it is mandatory to modify the $YAG:Ce^{3+}$ concentration for maintaining CCT values, resulting in many differences between the concentration and scattering capabilities of the structures.
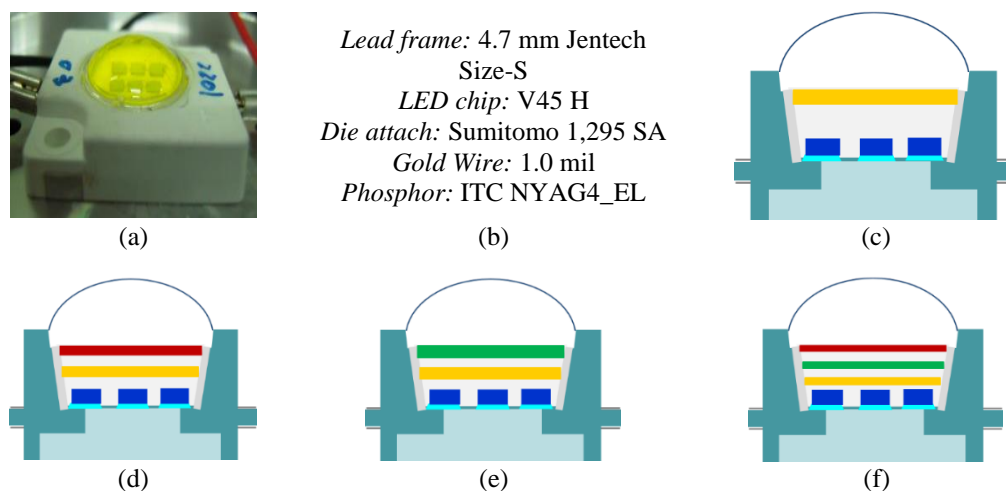
Figure 1. The schematic illustrations (a) the real-life WLED, (b) its parameters, (c) one-sheet remote phosphor structure, (d) two-sheet structure with red phosphor $CaO:Eu^{3+}$ (YR), (e) dual-layer structure with green phosphor $Zn_2SiO_4:Mn^{2+}$ (YG), and (f) three-sheet structure (YRG)

2.2. Making red and green-emitting substances

The phosphor creation process is a key factor needed to successfully simulate a WLED. The details of the red phosphor $CaO:Eu^{3+}$ and the green phosphor $Zn_2SiO_4:Mn^{2+}$ can be found in Tables 1 and 2 [21]. The procedure is demonstrated.

Table 1. Red-phosphor $CaCO_3:Eu^{3+}$ composition

Ingredient	Mole (%)	By weight (g)
$CaCO_3$	100	100
CaF_2	1.5	1.2
Eu_2O_3	1.2 (of Eu)	2.1

Table 2. Green-phosphor $Zn_2SiO_4:Mn^{2+}$ composition

Ingredient	Mole (%)	By weight (g)
ZnO	194	158
SiO_2	110	66
$MnCO_3$	6	6.9

We can begin the making of red phosphor $CaO_3:Eu^{3+}$ by combining the ingredients with water or methanol to acquire a slurry form. Once thoroughly mixed, the slurry is to be dried in the open air and subsequently pulverized. The powder acquired is to be heated thrice and pulverized every time heating is done. Note that there is a different condition for every heating. More specifically, for the first heating, the powder is placed in closed quartz pipes filled by N_2 and heated under 1,200 °C for 2 hours. For the second heating, replace the capped quartz boat with an open one, add N_2-infused H_2O to the boat, and heat it at 1,200 °C for 1 hour. The resulting substance is to be cooled to room temperature as fast as possible, then pulverized. For the third heating, the air is pumped into the quartz boat at 1,200 °C for approximately 20 minutes and then pulverized. Once more, the substance is cooled to room temperature and pulverized. The powder is to be stored dry in a carefully sealed container. The phosphor $CaO_3:Eu^{3+}$ has the red discharge hue discharge a discharge peak under 2.0.15 eV. For the creation of green phosphor $Zn_2SiO_4:Mn^{2+}$, the process begins with ball-milling the mixture of the ingredients in water for approximately 2 hours. The mixture is to be let dry in the open air, then pulverized. Heat the powder twice in open quartz containers at the temperature of 1,200 °C for 1 hour. Note that forming gas is used in the containers for the first heating, while air is used for the second heating instead. Pulverize the substance once the first heating is done. The green phosphor $Zn_2SiO_4:Mn^{2+}$ has a green discharge hue, discharge peak of 2.35 eV, along with discharge width of 0.18 eV. In order to acquire a proper understanding of how phosphor concentrations affect the optical characteristics of remote phosphor structures, we examined the changes in yellow phosphor concentrations at various CCTs in every structure (as seen in Figure 2). Judging the figure, we can see that at any CCT level, the concentration of yellow phosphor became largest for the one-layer Y structure and smallest for the three-layer YRG structure. The values of double-layer YR and YG are roughly similar. Overall, if we consider all structures to be made with the same CCT level, the structure with higher yellow phosphor concentration will have less lumen due to the increase in backscattering in the phosphor structures. Moreover, the higher the yellow phosphor concentration, the bigger the disparity between the colour distribution and the less uniformity of colour. Therefore, we can confirm that the YRG structure yields the best luminescence and colour quality for WLED. Judging the common ideas, the increase in the red spectrum of the white light emitted could result in better colour uniformity and CRI. The increased presence of the

green spectrum can help manipulate the luminescence efficiently. Because of this, examining the discharge spectrum for every phosphor package at certain CCTs would be crucial for assessing how they affect the quality of colour and the lumen efficacy in WLEDs. Figure 3 demonstrates results of the emission spectrum acquired at certain CCTs: 5,600; 6,600; 7,000; 7,700; and 8,500 K.

In the Y structure, the emission spectrum is at the lowest level, indicating the quality of colour and lumen output are lesser than those of other structures. In contrast, the three-layer remote phosphorus structure (YRG) appears to be more efficient than any others due to the fact that it generates the largest spectral density in the wavelength ranging from 380 to 780 nm, at all CCT values, see Figures 3(a)-(e) (in appendix). Furthermore, in terms of the two double-layer structures with a wavelength between 500 and 570 nm, the YG configuration appears to generate bigger emission intensity, resulting in higher lumen compared to the YR structure. While in the wavelength value between 650 and 750 nm for red colour, the YR configuration yields greater results, which offers advantages in the quality of colour, notably CRI of the WLED. The next part will present further details in our application of the Mie-dispersion hypothesis as well as Lambert-Beer principle for calculations to authenticate our discoveries.
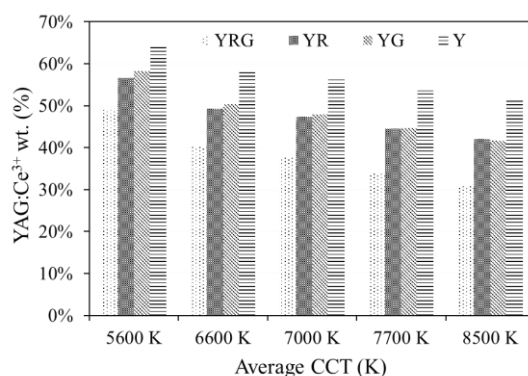

Figure 2. The concentration of yellow phosphor YAG:Ce^{3+} in different remote phosphor structures and color average correlated color temperatures (ACCTs)

3.   RESULTS AND DISCUSSION

Typically, general lighting applications require an illumination source with high luminescence and excellent chromatic reproduction. It is possible to calculate and determine the luminous efficiencies but the colour rendition that contributes greatly to promoting the chromatic reproduction efficiency is still up for debate. CRI has currently been the most applied color rendering standard. It is useful to briefly present the CRI definition as the basis of the evaluation. The CRI is introduced based on a colour comparison between the examined objects under the tested light source to that under the reference source. Thus, choosing the reference source is critical since it establishes the standard for the "real" colour of objects. The spectrum comparison between the tested light source and a black body radiator is also included in the introduction of CRI. When the temperature of the spectrum from the black body radiator is mostly close to that of the tested lighting source, this parameter is referred to the test source's CCT. Based on the CCT values of the tested source, the reference source mean is selected. When the test source's CCT goes beneath 5,000 K, a black body radiator having the similar CCT to the test source's is utilized to calculate the CRI. Above 5,000 K, the standard daylight spectrum with the same CCT, which is produced from a D65 standard illumination, is used. Among the fourteen samples of colour in use, the first eight samples are utilized for the measurement of general CRI values (R_a). The CRI has the advantage of being able to characterize the colour rendition performance of various light sources with a single number. Nonetheless, the CRI was proved to be deficient in colour rendering evaluation.

Figure 4 demonstrates the CRI of every remote phosphorus adjustment. As seen in Figure 4, at all CCTs levels, the YR configuration has the best CRI, while the YG structure has the worst CRI. The significant CRI enhancement in the YR formation would be possible thanks to the increased red spectral intensity caused by red phosphor CaO$_3$:Eu^{3+}. Furthermore, the CRI of WLED packages were improved at both lower and high CCT level in the YR structure. The task of improving the CRI of WLED at a high CCT level, such as 8,500 K, is incredibly challenging. Therefore, the practical utilization of double-layer remote phosphorus configuration in innovating WLED apparatuses greatly benefits from the outcome above. As previously stated, we examined the quality of color using two parameters: CRI (which is demonstrated) and

CQS. Figure 5 demonstrates the four structures' CQS. While the YRG structure has less CRI compared to the YR, it possesses the biggest CQS. Researchers have recently examined CQS and came to the conclusion that CQS is superior to CRI due to the fact that it uses three parameters (CRI, beholder's taste, and color coordinate) to assess the quality of color. Thanks to the color uniformity of the three primary chromas (blue, red, green), the YRG gives the best CQS.
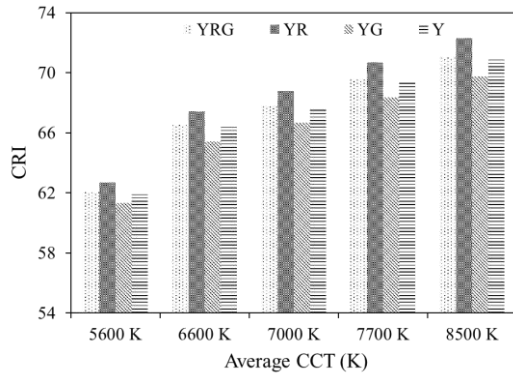

Figure 4. CRI values for phosphor settings under various ACCTs
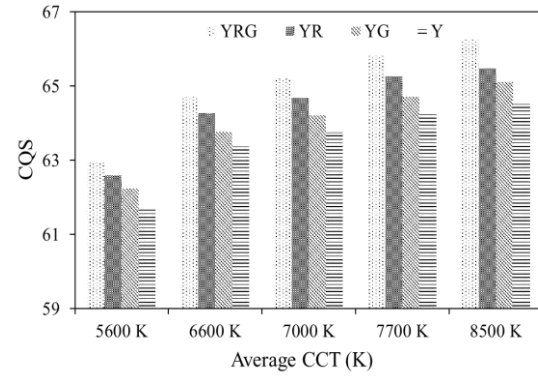
Figure 5. CQS of phosphor settings under various ACCTs

Considering the discoveries mentioned, the YRG structure appears to be the most suitable choice for improving the quality of colour in WLED thanks to its superior CRI and CQS values compared to the Y structure. Earlier research showed that the improvement of colour quality may lead to a sacrifice in the lumen output. From here, a matter of concern arises as we do not know if the YRG structure can suffer from this flaw or if we can parallelly enhance colour uniformity and luminescence. It is necessary to compare the lumen between the the one-layer (Y), double-layer (YG and YR), and three-layer (YRG) structures to solve the concern. The mathematical formulas were demonstrated with the basis of Mie-scattering theory to determine the value for propagated blue as well as transmuted yellow light within the structures. The calculations can help us verify the efficiency of extra phosphor layers in the WLED remote package in increasing optical efficacy.

The following formulas present the blue propagated blue as well as transmuted yellow illumination within the one-layered setting having the *2h*-breadth phosphor sheet [22]–[25]:

$$PY_1 = \frac{1}{2} \frac{\beta_1 \times PB_0}{\alpha_{B1} - \alpha_{Y1}} (e^{-2\alpha_{Y1}h} - e^{-2\alpha_{B1}h}) \tag{1}$$

$$PB_1 = PB_0 \times e^{-2\alpha_{B1}h} \tag{2}$$

In (3) and (4) are utilized to express the aforementioned lights of the double-layer structure with the *h*-thick phosphor layers:

$$PB_2 = PB_0 \times e^{-2\alpha_{B2}h} \tag{3}$$

$$PY_2 = \frac{1}{2} \frac{\beta_2 \times PB_0}{\alpha_{B2} - \alpha_{Y2}} (e^{-2\alpha_{Y2}h} - e^{-2\alpha_{B2}h}) \tag{4}$$

In (5) and (6) present the aforementioned lights of the three-layer structure with phosphor layers at $\frac{2h}{3}$ hickness:

$$PB_3 = PB_0 . e^{-\alpha_{B2}\frac{2h}{3}} . e^{-\alpha_{B2}\frac{2h}{3}} . e^{-\alpha_{B2}\frac{2h}{3}} = PB_0 . e^{-2\alpha_{B3}h} \tag{5}$$

$$PY'_3 = \frac{1}{2} \frac{\beta_3 PB_0}{\alpha_{B3} - \alpha_{Y3}} [e^{-\alpha_{Y3}\frac{2h}{3}} - e^{-\alpha_{B3}\frac{2h}{3}}] e^{-\alpha_{Y3}\frac{2h}{3}} + \frac{1}{2} \frac{\beta_3 PB_0 e^{-\alpha_{B3}\frac{2h}{3}}}{\alpha_{B3} - \alpha_{Y3}} [e^{-\alpha_{Y3}\frac{2h}{3}} - e^{-\alpha_{B3}\frac{2h}{3}}] \tag{6}$$
$$= \frac{1}{2} \frac{\beta_3 PB_0}{\alpha_{B3} - \alpha_{Y3}} [e^{-\alpha_{Y3}\frac{4h}{3}} - e^{-2\alpha_{B3}\frac{4h}{3}}]$$

The superiority of the three-layer structure in optical efficiency compared to the double-layer could be inferred from (7):

$$\frac{(PB_3 - PY_3) - (PB_2 + PY_2)}{(PB_2 + PY_2)} > \frac{e^{-2\alpha_{B_3}h} - e^{-2\alpha_{B_2}h}}{e^{-2\alpha_{Y_3}h} - e^{-2\alpha_{B_2}h}} > 0 \qquad (7)$$

For all the formulas demonstrated in (1)-(7), h is counted as the phosphor-sheet thickness. One-layer, double-layer, and three-layer settings will be indicated by subscripts "1", "2", and "3". β describes the converting efficiency of light beams from blue into yellow. γ describes the the reflection efficiency for the yellow illumination. PB and PY represent the blue as well as yellow illumination' intensities. The symbol PB_0, comprising PB as well as PY, indicates the intensity of light in blue LED. Both α_B and α_Y are the symbols showing the blue- and yellow-light energy loss in transmission and conversion within the remote phosphor packet. Furthermore, the yellow illumination bypassing the two layers of red as well as green phosphors is indicated by the symbol PY'_3 in (6). Moreover, we can see that in Figure 6, the YRG structure yielded the greatest lumen output at all temperatures of color. The Y structure, on the contrary, yielded the smallest lumen output, see Figure 6. On the other hand, the double-layer structure with the layer of green phosphor $Zn_2SiO_4:Mn^{2+}$ (YG) demonstrates effective manipulation of lumen efficacy due to its luminescence being second only to the YRG, thanks to greater green spectral energy (500-570 nm) in the allocation of white-light spectral power. Also in the figure, we can see that the green spectral zone in the YRG structure yielded greater intensity than any other structures and hence the greater lumen in YRG than other structures. Specifically, the presence of green as well as red illumination generated by the green phosphor $Zn_2SiO_4:Mn^{2+}$ and red phosphor $CaO:Eu^{3+}$ can improve the scattering process and color uniformity. The said structure also kept a significant amount of light backscattering towards the LED chip as low as possible. The lumen output, as a result, is improved by the greater propagation of light. We should note that configuring the phosphor layers' concentration is necessary to achieve the greatest energy transmission. This is proven by (7) (based on Lambert-Beer law). In order to further authenticate the YRG's efficiency in improving WLED's quality of color, the color correlated temperature deviation (D-CCT) of every structure was examined. The D-CCT values of the structures acquired are shown in Figure 7.
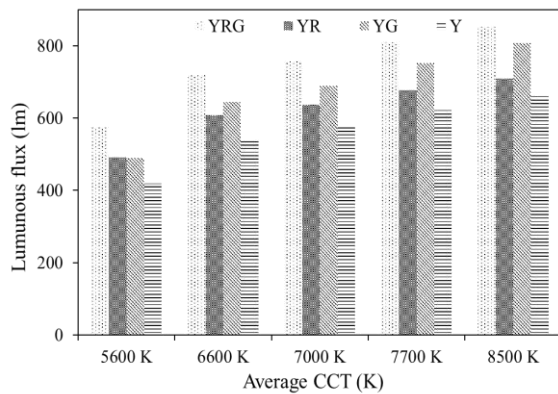

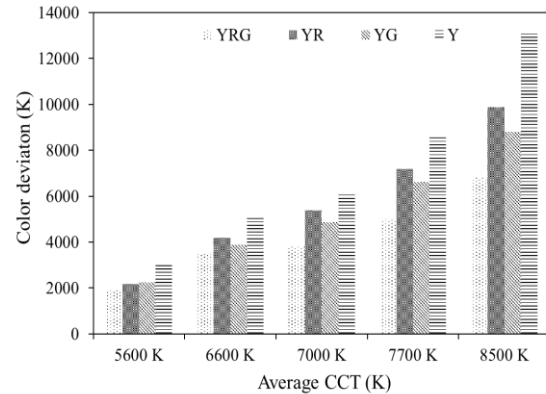Figure 6. Lumen output for phosphor settings under various ACCTs

Figure 7. The D-CCTs of phosphor settings under various ACCTs

YRG is shown to have the smallest D-CCT, regardless of CCTs. The YRG's enhanced scattering characteristics result in better quality of color. As we can see here, adding more layers of phosphor will increase the scattering of light, resulting in a more efficient mixing process of light prior to the creation of white light, and hence the better color uniformity can be accomplished. It should be noted that the lumen will decrease whenever the scattering increases. Fortunately, the said reduction appears to be remarkably low and should be considered a reasonable sacrifice for a noticeably better quality of color, while the lumen is kept at relatively high levels when using the YRG structure. For manufacturers, the three-layer remote phosphor structure can be a huge benefit to the WLED's quality.

4.   CONCLUSION

This research compared the optical performance for the one-layer (Y), double-layer (YG and YR), and three-layer (YRG) structures for the purpose of selecting the best structure possible that can be used for the innovation of WLED. For the recreation of WLED samples, we utilized the green phosphor Zn_2SiO_4:Mn^{2+} and the red phosphor CaO:Eu^{3+}. Our assessment and authentication of the results after measurements were based on the Mie dispersion hypothesis as well as Lambert-Beer principle. Because of the red phosphor's significance in increasing the presence of red light in the white-light spectrum, we found that the YR structure is best employed to improve WLED's CRI. The YG structure can be used to achieve higher lumen thanks to the increased presence of green spectral light. The YRG structure yielded the second-best CRI, best CQS value as well as the best lumen efficacy of all structures tested at all CCT levels. On the other hand, its color deviation has the lowest value of all, resulting in the highest color homogeneity. After a thorough comparison, it is no doubt that YRG should be considered the best remote phosphor structure for the purpose of manufacturing WLED with better quality.

APPENDIX
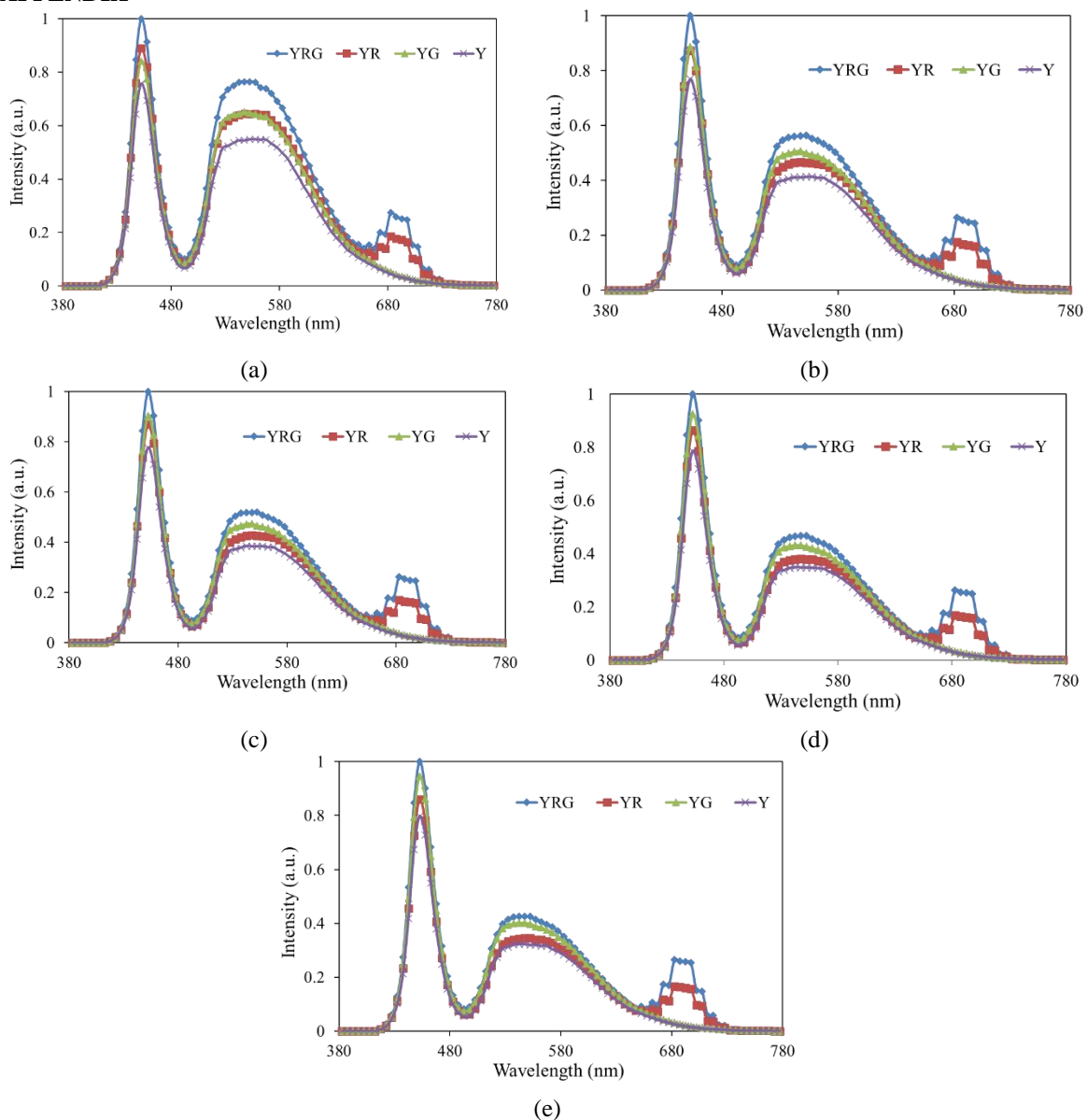

(a)

(b)

(c)

(d)

(e)

Figure 3. The emitting spectrum for each remote phosphor structure at different ACCTs (a) 5,600 K, (b) 6,600 K, (c) 7,700 K, (d) 7,700 K, and (e) 8,500 K

REFERENCES

[1] Z. Zhang and W. Yang, "Tunable photoluminescence in $Ba_{1-x}SrxSi_3O_4N_2$: Eu^{2+}/Ce^{3+}, Li^+solid solution phosphors induced by linear structural evolution," *Optical Materials Express*, vol. 9, no. 4, pp. 1922–1932, Apr. 2019, doi: 10.1364/OME.9.001922.

[2] T. W. Kang *et al.*, "Enhancement of the optical properties of $CsPbBr_3$ perovskite nanocrystals using three different solvents," *Optics Letters*, vol. 45, no. 18, pp. 4972–4975, Sep. 2020, doi: 10.1364/OL.401058.

[3] G. Prabhakar, P. Gregg, L. Rishoj, P. Kristensen, and S. Ramachandran, "Octave-wide supercontinuum generation of light-carrying orbital angular momentum," *Optics Express*, vol. 27, no. 8, pp. 11547–11556, Apr. 2019, doi: 10.1364/OE.27.011547.

[4] R. Dang, H. Tan, N. Wang, G. Liu, F. Zhang, and X. Song, "Raman spectroscopy-based method for evaluating LED illumination-induced damage to pigments in high-light-sensitivity art," *Applied Optics*, vol. 59, no. 15, pp. 4599–4605, May 2020, doi: 10.1364/AO.379398.

[5] H. -L. Ke *et al.*, "Lumen degradation analysis of LED lamps based on the subsystem isolation method," *Applied Optics*, vol. 57, no. 4, pp. 849–854, Feb. 2018, doi: 10.1364/AO.57.000849.

[6] S. Sadeghi, B. G. Kumar, R. Melikov, M. M. Aria, H. B. Jalali, and S. Nizamoglu, "Quantum dot white LEDs with high luminous efficiency," *Optica*, vol. 5, no. 7, pp. 793–802, Jul. 2018, doi: 10.1364/OPTICA.5.000793.

[7] T. Wang, "Electrically injected hybrid III-nitride/organic white LEDs with nonradiative energy," in *2018 Conference on Lasers and Electro-Optics Pacific Rim (CLEO-PR)*, 2018, pp. 1–2, doi: 10.1364/CLEOPR.2018.W2J.1.

[8] C. Zhang, L. Xiao, P. Zhong, and G. He, "Photometric optimization and comparison of hybrid white LEDs for mesopic road lighting," *Applied Optics*, vol. 57, no. 16, pp. 4665–4671, Jun. 2018, doi: 10.1364/AO.57.004665.

[9] X. Li *et al.*, "Highly stable and tunable white luminescence from Ag-Eu^{3+} co-doped fluoroborate glass phosphors combined with violet LED," *Optics Express*, vol. 26, no. 2, pp. 1870–1881, Jan. 2018, doi: 10.1364/OE.26.001870.

[10] W. Shiyu, S. Yan, and Z. Yi, "Color temperature adjustable LED based on structured fluorescent film," in *2018 Asia Communications and Photonics Conference (ACP)*, Oct. 2018, pp. 1–3, doi: 10.1109/ACP.2018.8595763.

[11] X. Bao, X. Gu, and W. Zhang, "User-centric quality of experience optimized resource allocation algorithm in VLC network with multi-color LED," *Optics Express*, vol. 26, no. 21, pp. 27826–27841, Oct. 2018, doi: 10.1364/OE.26.027826.

[12] Z. Huang *et al.*, "Towards an optimum colour preference metric for white light sources: a comprehensive investigation based on empirical data," *Optics Express*, vol. 29, no. 5, pp. 6302–6319, Mar. 2021, doi: 10.1364/OE.413389.

[13] S. Ma, P. Hanselaer, K. Teunissen, and K. A. G. Smet, "Effect of adapting field size on chromatic adaptation," *Optics Express*, vol. 28, no. 12, pp. 17266–17285, Jun. 2020, doi: 10.1364/OE.392844.

[14] P. Kaur, Kriti, Rahul, S. Kaur, A. Kandasami, and D. P. Singh, "Synchrotron-based VUV excitation-induced ultrahigh quality cool white light luminescence from Sm-doped ZnO," *Optics Letters*, vol. 45, no. 12, pp. 3349–3352, Jun. 2020, doi: 10.1364/OL.395393.

[15] D. Yan, S. Zhao, H. Wang, and Z. Zang, "Ultrapure and highly efficient green light emitting devices based on ligand-modified $CsPbBr_3$ quantum dots," *Photonics Research*, vol. 8, no. 7, pp. 1086–1092, Jul. 2020, doi: 10.1364/PRJ.391703.

[16] J. Cheng *et al.*, "Luminescence and energy transfer properties of color-tunable $Sr_4La(PO_4)_3O$: Ce^{3+}, Tb^{3+}, Mn^{2+} phosphors for WLEDs," *Optical Materials Express*, vol. 8, no. 7, pp. 1850–1862, Jul. 2018, doi:. 10.1364/OME.8.001850

[17] Z. Zhao, H. Zhang, S. Liu, and X. Wang, "Effective freeform TIR lens designed for LEDs with high angular color uniformity," *Applied Optics*, vol. 57, no. 15, pp. 4216–4221, May 2018, doi: 10.1364/AO.57.004216.

[18] Z. Wen *et al.*, "Fabrication and optical properties of Pr^{3+}-doped Ba (Sn, Zr, Mg, Ta) O_3 transparent ceramic phosphor," *Optics Letters*, vol. 43, no. 11, pp. 2438–2441, Jun. 2018, doi: 10.1364/OL.43.002438.

[19] C. J. C. Smyth, S. Mirkhanov, A. H. Quarterman, and K. G. Wilcox, "275 W/m^2 collection efficiency solar laser using a diffuse scattering cooling liquid," *Applied Optics*, vol. 57, no. 15, pp. 4008–4012, May 2018, doi: 10.1364/AO.57.004008.

[20] Z. Song, T. Guo, X. Fu, and X. Hu, "Residual vibration control based on a global search method in a high-speed white light scanning interferometer," *Applied Optics*, vol. 57, no. 13, pp. 3415–3422, May 2018, doi: 10.1364/AO.57.003415.

[21] C. McDonnell, E. Coyne, and G. M. O'Connor, "Grey-scale silicon diffractive optics for selective laser ablation of thin conductive films," *Applied Optics*, vol. 57, no. 24, pp. 6966–6970, Aug. 2018, doi: 10.1364/AO.57.006966.

[22] S. -R. Chung, C. -B. Siao, and K. -W. Wang, "Full color display fabricated by CdSe bi-color quantum dots-based white light-emitting diodes," *Optical Materials Express*, vol. 8, no. 9, pp. 2677–2686, Sep. 2018, doi: 10.1364/OME.8.002677.

[23] J. Zhang, L. Zhao, X. Bian, and G. Chen, "Ce^{3+}/Mn^{2+}-activated Ca_7 $(PO_4)_2(SiO_4)_2$: efficient luminescent materials for multifunctional applications," *Optics Express*, vol. 26, no. 18, pp. 904–914, Sep. 2018, doi: 10.1364/OE.26.00A904.

[24] T. Kozacki, M. Chlipala, and H. -G. Choo, "Fourier rainbow holography," *Optics Express*, vol. 26, no. 19, pp. 25086–25097, Sep. 2018, doi: 10.1364/OE.26.025086.

[25] C. Han *et al.*, "Effect of surface recombination in high performance white-light $CH_3NH_3PbI_3$ single crystal photodetectors," *Optics Express*, vol. 26, no. 20, pp. 26307–26316, Oct. 2018, doi: 10.1364/OE.26.026307.

BIOGRAPHIES OF AUTHORS

Ho Minh Trung received the Ph.D. degree in physics from University of Science, Vietnam National University Ho Chi Minh City, Vietnam. He is working as a lecturer at the Faculty of Basic Sciences, Vinh Long University of Technology Education, Vietnam. His research interests focus on developing the patterned substrate with micro-and nano-scale to apply for physical and chemical devices such as solar cells, OLED, and photoanode. He can be contacted at email: trunghm@vlute.edu.vn.

My Hanh Nguyen Thi received a Bachelor of Physics from An Giang University, Vietnam, Master of Theoretical Physics and Mathematical Physics, Hanoi National University of Education, Vietnam. Currently, she is a lecturer at the Faculty of Mechanical Engineering, Industrial University of Ho Chi Minh City, Vietnam. Her research interests are theoretical physics and mathematical physics. She can be contacted at email: nguyenthimyhanh@iuh.edu.vn.

Hoang Thinh Nhan received his Engineer Diploma in Mechanical Engineering (Industrial Machines, Equipment and Process) from Ufa State Petromeum Technology University (USPTU), Russia, in 2003 and Ph.D. degree in Mechanical Engineering from USPTU in 2006. He is currently working as Deputy Director of Center of Innovation and Business Incubation in the Nguyen Tat Thanh University, Ho Chi Minh City, Vietnam. His research interests include renewable energy, optimisation techniques, hydraulic and pneumatic systems, and offshore engineering. He can be contacted at email: htnhan@ntt.edu.vn.